THE ROLE OF CRYSTALLISATION ON THE SWITCHING OF GLASSES IN THE SYSTEM SiO_2–B_2O_3–Bi_2O_3–Na_2O

A Thesis Submitted
in Partial Fulfilment of the Requirements
for the Degree of
MASTER OF TECHNOLOGY

By
MADHUSHREE SINGH

to the

INTERDISCIPLINARY PROGRAMME IN MATERIALS SCIENCE
INDIAN INSTITUTE OF TECHNOLOGY KANPUR
AUGUST, 1976

CERTIFICATE

This is to certify that this work on "The Role of Crystallisation in the Switching of Glasses in the System SiO_2-B_2O_3-Bi_2O_3-Na_2O" by Madhushree Singh has been carried out under my supervision and has not been submitted elsewhere for a degree.

D. Chakravorty

D. CHAKRAVORTY
Professor
Department of Metallurgical Engineering
Indian Institute of Technology, Kanpur

ACKNOWLEDGEMENTS

I owe a deep gratitude to Professor D. Chakravorty for his encouragement and excellent guidance throughout this work.

I am thankful to Dr. E.C. Subbarao and Dr. R. Sharan for their encouragement and inspiration.

My sincere thanks are due to all the people who have helped me in my experimental work at every stage.

The financial support of Pilkington Brothers Ltd., U.K. is gratefully acknowledged.

Madhushree Singh

CONTENTS

		Page
	LIST OF FIGURES	(vi)
	SYNOPSIS	(viii)
CHAPTER I	INTRODUCTION	1
1.1	Amorphous Semiconductor Materials	1
1.2	Semiconducting Properties	3
1.3	Band Model	4
1.4	Electronic Conduction of Oxide Glasses	6
1.5	Ionic Conductivity of Oxide Glasses	9
1.6	Glass Switches	9
1.7	Mechanisms of Switching	10
1.8	Switching in Borate Glasses Containing Bi_2O_3	12
CHAPTER II	STATEMENT OF THE PROBLEM	15
CHAPTER III	EXPERIMENTAL DETAILS	16
3.1	Base Glass Preparation	16
3.2	Crystallisation of the Glasses	17
3.3	Specimen Preparation for Resistivity Measurements	17
3.4	Resistivity Measurements	18
3.5	Preparation of Samples for X-ray Diffraction Studies	18
3.6	Resistance Measurements on $Bi_2O_3.3B_2O_3$ Samples	19
3.7	Sample Preparation for D.T.A. Analysis	20

		Page
CHAPTER IV	RESULTS AND DISCUSSIONS	21
4.1	Resistivity Measurements on Glasses	21
4.2	X-Ray Diffraction Data	24
4.3	Resistivity Measurements on $Bi_2O_3.3B_2O_3$ Specimens	26
CHAPTER V	CONCLUSIONS AND PROPOSALS FOR FURTHER WORK	28
CHAPTER VI	LIST OF TABLES	31
	REFERENCES	42

LIST OF FIGURES

1.1 Band structure in
(a) ordered imperfect crystal
(b) disordered material.

1.2 The mobility gap.

1.3 Classification of switching characteristics

3.1 Sample holder for resistivity measurements

3.2 Circuit diagram for resistivity measurement

3.3 Circuit diagram for resistivity measurement with VTVM

3.4 Set-up for low temperature resistivity measurement

4.1 Plot of log resistivity versus 1/T for glass no. 1

4.2 Plot of log resistivity versus 1/T for glass no. 3

4.3 Plot of log resistivity versus 1/T for glass no. 4

4.4 Plot of log resistivity versus 1/T for glass no. 5

4.5 Plot of log resistivity versus 1/T for crystallised glass no. 2

4.6 Plot of log resistivity versus 1/T for crystallised glass no. 3

4.7 Plot of log resistivity versus 1/T for crystallised glass no. 4

4.8 X-ray diffraction patterns for crystallised glasses no. 1, 2 and 3 and virgin glasses no. 1 and 2

4.9 X-ray diffraction patterns for crystallised glass no. 1 and $Bi_2O_3.3B_2O_3$ sample

4.10 V-I characteristics of $Bi_2O_3.3B_2O_3$ sample no. 1 in OFF-state

4.11 V-I characteristic of $Bi_2O_3.3B_2O_3$ sample no. 1 in ON-state

4.12 Log resistivity versus 1/T characteristics for $Bi_2O_3.3B_2O_3$ sample no. 1

4.13 V-I characteristic of $Bi_2O_3.3B_2O_3$ sample no. 2 in the ON-state

4.14 Log resistivity versus 1/T plot for $Bi_2O_3.3B_2O_3$ sample no. 2

4.15 DTA curve for glass sample no. 1

4.16 DTA curve for glass sample no. 4

4.17 DTA curve for glass sample no. 5

SYNOPSIS

Memory switching has been observed in the surface layers of Na_2O-B_2O_3-Bi_2O_3-SiO_2 glasses which have been subjected to $Na^+ \rightleftharpoons Ag^+$ ion exchange followed by reduction treatment in hydrogen. Some of the glasses showed a tendency to crystallise on preparation. It was proposed to find exactly what role crystallisation played in the switching of the glass. In order to do this resistivity characteristics of the bulk parent glass and crystallised glasses were studied. The crystalline phase precipitated was identified by X-ray methods. The electrical properties of the crystalline phase were studied, by synthetically preparing the ceramic sample in the lab. The crystalline phase itself showed switching at a lower level of resistance but of the same order of magnitude as the parent glass. Low temperature measurements on the sample showed a metallic behaviour when the sample was in the ON-state.

CHAPTER I

INTRODUCTION

1.1 Amorphous Semiconductor Materials

The standard glasses we meet in everyday life are based mostly on silicon oxide, boric oxide or lead oxide. Such glasses generally conduct by ion movement, and have no relevance to our work. Our interest is shared between two classes of amorphous materials, the amorphous form of the standard semiconductors like Ge and Si, and certain glasses which have semiconducting properties.

The interest in amorphous Ge, Si and III-V compounds arises because we hope that we can learn something about the physics of the amorphous state by similarities between and differences from the properties of single crystals of the same materials. This process of extrapolation has had a limited success, but it is difficult to get data which is truly representative of amorphous semiconductors because the properties depend markedly on the method of preparation. Selenium is perhaps the one amorphous semiconductor which can be readily studied in both amorphous and crystalline form and indeed has device application in both forms, amorphous Se being used in

Xerography and crystalline Se for photocells. Glassy selenium is readily denitrified by heating but its stability is improved by the addition of either As or Ge. The effect is however reversed if the proporties exceeds 60% or the Ge proportion 30%. These binary systems are true semiconductor glasses, and have many points in common with the more complex systems which are now the object of detailed study because of their device potential. Hundreds of combination of over 20 elements have semiconducting properties, but most promise appears to be shown by glasses based on elements from the VIth group the chalcogenide glasses.

Though the chalcogenides are thought by most laboratories to have the greatest device possibility, they do have the disadvantage of low maximum temperature of device operation. There is, therefore, some interest in glasses made with different glasses formers and of these the metal oxides have received most attention. Among these are iron phosphates, copper phosphates and vanadium phosphates. Vanadium oxide alone can be prepared as a glass, and in addition can be mixed with tellunium oxide or barium oxide. The chemistry of the oxide systems is more complex than that of the chalcogenides. Ions can exist in several valence states, and the thermal treatments and melt atmosphere must be controlled

accurately to achieve reproducible glasses.

The more complex chalcogenide and oxide glasses are difficult to prepare as homogeneous uniform materials. Often there is a two-phase structure, and sometimes one of the phases is crystalline. Some glasses show a sub-structure of tiny drops a micron or so in diameter. It is not then sufficient to know the composition of the glass under examination – one must also know the degree of crystallinity and homogeneity.

1.2 Semiconducting Properties

Glasses have a high resistivity compared with the standard semiconductors. At room temperature the resistivity can be as high as 10^{16} ohm-cm. For As_2S_5 or as low as 100 ohm-cm for GeTe. Small quantities of impurity have little effect on the conductivity of most amorphous materials. It is likely that impurity here does not create impurity levels but reduces disorder in the glass.

All glasses show an increase in conductivity with temperature, and in chalcogenides there is a simple exponential variation with 1/T for an appreciable temperature range near room temperature. The behaviour has some similarities to an intrinsic semiconductor. In some other amorphous materials there are two or three

activation energies over a temperature range of several hundred degrees.

Mobilities are universally low, and often it is difficult to establish even the sign of the Hall coefficient. Where it can be measured, it is negative, on the other hand the thermo-electric power is nearly always positive.

Glasses are non-ohmic. The current increases more rapidly than the field for fields greater than 10^4 volts/cm. There is the possibility, at least in thin films, of electrode effects, giving carrier injection, space-charge growth to finally space-charge limited currents. In many experiments electrode effects are eliminated but large non-ohmic effects are still observed. It is generally accepted that these effects are due to Poole-Frenkel mechanism, a lowering of a coulombic barrier by the electric field. The field F lowers the ionisation energy of the centre by $2 Fe^3/K$. This amount of barrier reduction would occur in the absence of tunneling. At low temperatures tunnel currents will give an additional field dependent contribution.

1.3 Band Model

In the past three years there has been a coalescence of views on the band structure of amorphous

semiconductors. Different authors however arrive at similar end-points after following a variety of paths. We consider here the 3 main paths. Cohen, Fritzsche and Oveshinsky (1) develop their model by considering an imperfect crystal as an intermediate state between the perfect crystal and the disordered solid. For a perfect crystal the density of states has band edges which are sharp, square root singularities within the bands, and distinct energy separations between the upper boundary of one band and the lower boundary of the next band. Each localised imperfection which gives a large change in crystal potential creates a localised bound state in the gap between the two bands. Additional imperfections give extra bound states, and if there are a large number of imperfections the bound states become a subsidiary band within the energy gap. The square root singularities within the main bands are by now rounded off, but the sharp edges remain. As the crystal perfection decreases, still more the subsidiary bands within the energy gap merge with the main bands, giving tails of localised states continuous with the band of extended states. This could well represent the band structure of amorphous germanium. A more complex material, such as a chalcogenide, can show compositional disorder as well as structural disorder. The tail states

will now be more pronounced, and the upper energy tail from one band may overlap with the lower energy tail of the next band giving localised states throughout the 'forbidden gap'. The Fermi level will be within the region of overlap, and the valence band states above the Fermi level will empty and operate as electron traps. Similarly the conduction band states below the Fermi level will become hole traps. This is shown in Fig. 1.1.

Though there are now allowed states at all energies, the nature of the states changes with energy. A carrier in the localised states moves by phonon-assisted hopping and its mobility is therefore low. In the extended states the carriers will be subjected to a number of scattering processes but their mobility will be 2 or 3 orders of magnitude greater. The mobility is therefore a function of energy, showing a steep change at energies corresponding to the previous conduction and valence band edges. A valence band gap therefore replaces the density of states gap, as shown in Fig. 1.2. Further references on this topic are Ref. (2-6).

1.4 Electronic Conduction of Oxide Glasses

In 1957, Baynton et al (7) first reported that a family of glasses based on V_2O_5 and P_2O_5 was

semiconducting rather than ionically conducting. Some years later, because of the need of semiconductors with fairly high electrical resistivity (e.g. 10^{12} ohm cm at 20°C) that are easily fabricated into intricate shapes, these semiconducting glasses were actively studied.

That long range order is not a prerequisite for metallic conduction is easily demonstrated from the observed electrical properties of liquid metals. For V_2O_5 an n-type semiconductor the electrical conductivity increases gradually as the crystal is heated, and no sharp variation is observed when melting occurs (8). It appears that long-range order is also not a prerequisite for electronic conduction in semiconducting oxides.

The conductivity of all semiconducting glasses studied so far increases with increasing temperature. From room temperature to near the glass-transition temperatures the simple expression

$$\sigma = \sigma_o \exp(-\frac{E}{kT})$$

apparently holds. The activation energy E is usually much less than the band-gap energy of the particular crystalline transition metal oxide used in the glass.

Theoretical treatments by Mott (9) and Austin and Mott (10) have been successful in explaining the qualitative temperature dependence of conductivity of semiconducting oxide glasses at low temperatures. Mott considers the mechanism of conduction in these glasses to be similar to that for impurity conduction in doped and compensated crystalline semiconductors at low temperatures, example in germanium. In germanium the predominant activation energy. E_D controls the process of electron tunneling between occupied and empty donors. In polar oxides where an extra electron can cause distortion around a charge center, an additional activation energy E_H must be considered.

(E_D – Miller-Abraham activation energy

E_H – polaron-hopping activation energy)

E_H is more important in oxide glasses. Mott proposed that electronic conductivity should be described by

$$\sigma = \nu C(1 - C) \frac{e^2}{RkT} \exp(-2\beta R) \exp(-\frac{W}{kT})$$

where $W = \frac{1}{2} W_D + W_H$

C, (1-C) are the concentration of ions in the two valence states respectively

ν is the phonon frequency

β is the rate of decay of a wave function

R is the mean distance between the ions.

It was predicted by Mott that W tends to zero as T approaches zero, thus giving a decreasing slope of the ln σ versus 1/T plot.

1.5 Ionic Conductivity of Oxide Glasses

The motion of alkali ions, in particular sodium ions, is by far the most important mechanism of ionic conductivity in oxide glasses (Stevel's model).

For most oxide glasses, over a fairly wide temperature range, the electrical resistivity ρ is described by the Rasch-Hinrichsen relation.

$$\log \rho = A + \frac{B}{T}$$

where A and B are constants. However in the presence of fairly small amounts of transition metal-oxides, electronic conductivity predominates

1.6 Glass Switches

Ovshinsky (12,13) observed switching in amorphous semiconductors for the first time in the Te-As-Si-Ge system. Two main types of glass switch, with

characteristics illustrated in Fig. 1.3 are the threshold switch and the memory switch sometimes called monostable and bistable switches respectively. The threshold switch shows a high resistance at voltages below a critical value V_T, at which it changes to a conducting state. This threshold voltage is almost proportional to electrode separation, but varies with glass composition.

The memory switch similarly has a resistance state and a threshold voltage, but the conducting state is maintained even when the bias is removed. The device is returned to the high resistance state by the passage of a short high current pulse. Both threshold and memory switches have symmetrical current-voltage characteristics which are shown in figures 1.3a and 1.3b respectively.

1.7 Mechanisms of Switching

Two possible explanations for the switching behaviour have been given

(1) thermal mechanism of Pearson, Boer, Kaplan and Adler

(2) electronic mechanism by Henisch and Pryor.

1.7.1 Thermal mechanism

This mechanism (14-19) suggests that the memory effect is explanable by a phase change process. The

passage of large currents in the OFF state of the switch result in enough joule heating to allow phase change to occur. If the new phases are crystalline, have high conductivity and extend continuously between the electrodes then they can form a stable conducting path giving rise to the ON state. The mechanism of switching off can be explained as follows. Passage of a critically large current pulse in the memory state (ON) would result in the fusion of 'hot-spots' along this path. If the current ceased abruptly these fused regions would be quenched to the glassy state, then the device would be off due to the high resistance. Slow cessation of current flow would result in slow cooling of the fused hot-spots with recrystallisation to reform the continuous conducting path. Thus under these conditions the device would remain in the memory state.

1.7.2 Electronic model

This model was proposed by Henish and Pryor (20) and Van Roosbroock. The electronic model suggests that a double injection space charge processes is taking place within the material. A neutral plasma thus produced, creates an instability which is propagated through the material resulting in a voltage drop across

the device and the observed S-shaped negative resistance in the switch characteristic. Electronic mechanisms may be polar or non-polar to experimental results show that both prevail.

The validity of the above model has however been questioned recently by Thomas and Bosnell (21) who have studied thin film switches of the Si-Ge-Te-As system.

1.8 Switching in Borate Glasses Containing Bi_2O_3

Memory switching has been observed in the surface layers of Na_2O-B_2O_3-Bi_2O_3-SiO_2 glasses which have been subjected to $Na^+ \rightleftharpoons Ag^+$ ion exchange followed by reduction treatment in hydrogen. Switching is from 10^9 ohm off-state to 10^3 ohm on-state (22). It is proposed to find a possible mechanism for this phenomenon.

The virgin specimens have a microstructure which consists of metallic bismuth particles with diameters ranging 50 to 250 Å. After ion exchange and reduction silver particles of maximum diameter 700 Å were precipitated in the glass matrix. Chakravorty (23) has tentatively suggested that switching might occur because of the crystallisation process induced in the glass phase between the metallic particles.

In order to test the validity of this explanation, the d.c. behaviour of Na_2O-B_2O_3-Bi_2O_3-SiO_2 glass film was studied without subjecting it to any ion exchange and reduction treatment. The precipitation of metallic silver in the glass matrix was thereby avoided (23).

Negative resistance regions were obtained in these specimens. Resistance levels of the two states are 10^6 ohm and 3 ohm respectively. These glasses tend to crystallise in the temperature range 500-600°C and the crystalline phase has a lower resistance than the parent glass. The switch off temperature is found to be close to the melting point of metallic bismuth.

Thus if it is assumed that the on-state is a result of the formation of bismuth filaments between the conducting islands the switch-off process could be explained on the basis of a rupture of the filaments in a manner similar to a fuse blowing (23).

In chalcogenide glasses showing memory action switching has been ascribed to crystalline conducting phase formation (14-17). Some of the glasses in the system Na_2O-B_2O_3-Bi_2O_3-SiO_2 have shown devitrification tendencies during preparation (24). Microstructures of these glasses have shown the presence of a crystalline phase. Precipitation of such a phase could cause memory

switching in these glass systems if the crystalline phase has a lower value of resistance than the parent glass.

On the other hand Chakravorty (22) studying the same system has postulated that the switching action is due to formation of conducting islands of bismuth in the glassy matrix. In the off-state conduction could arise from electron hopping between conducting islands of bismuth. Microstructures of certain glasses studied have shown metallic bismuth particles of varying diameters upto 250 Å. Which of these two mechanisms actually gives rise to switching has to be investigated.

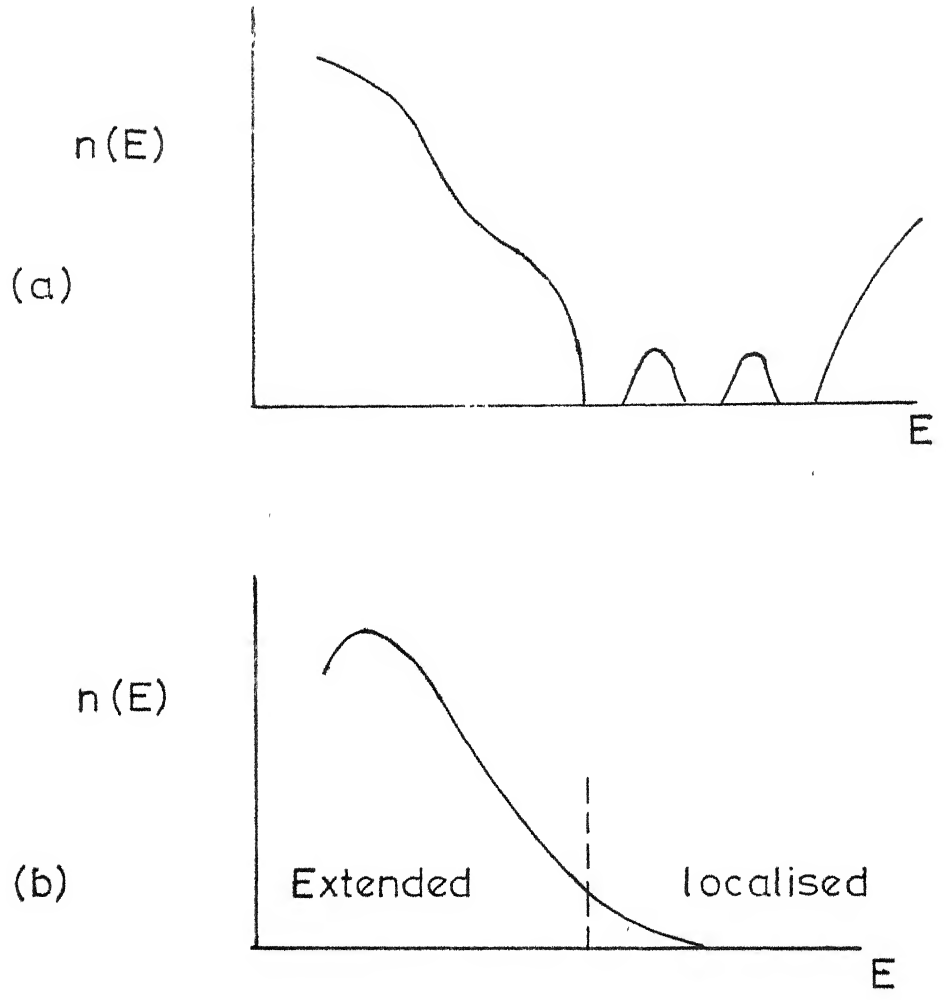

FIG.1.1 BAND STRUCTURE IN

(a) ORDERED IMPERFECT CRYSTAL.

(b) DISORDERED MATERIAL.

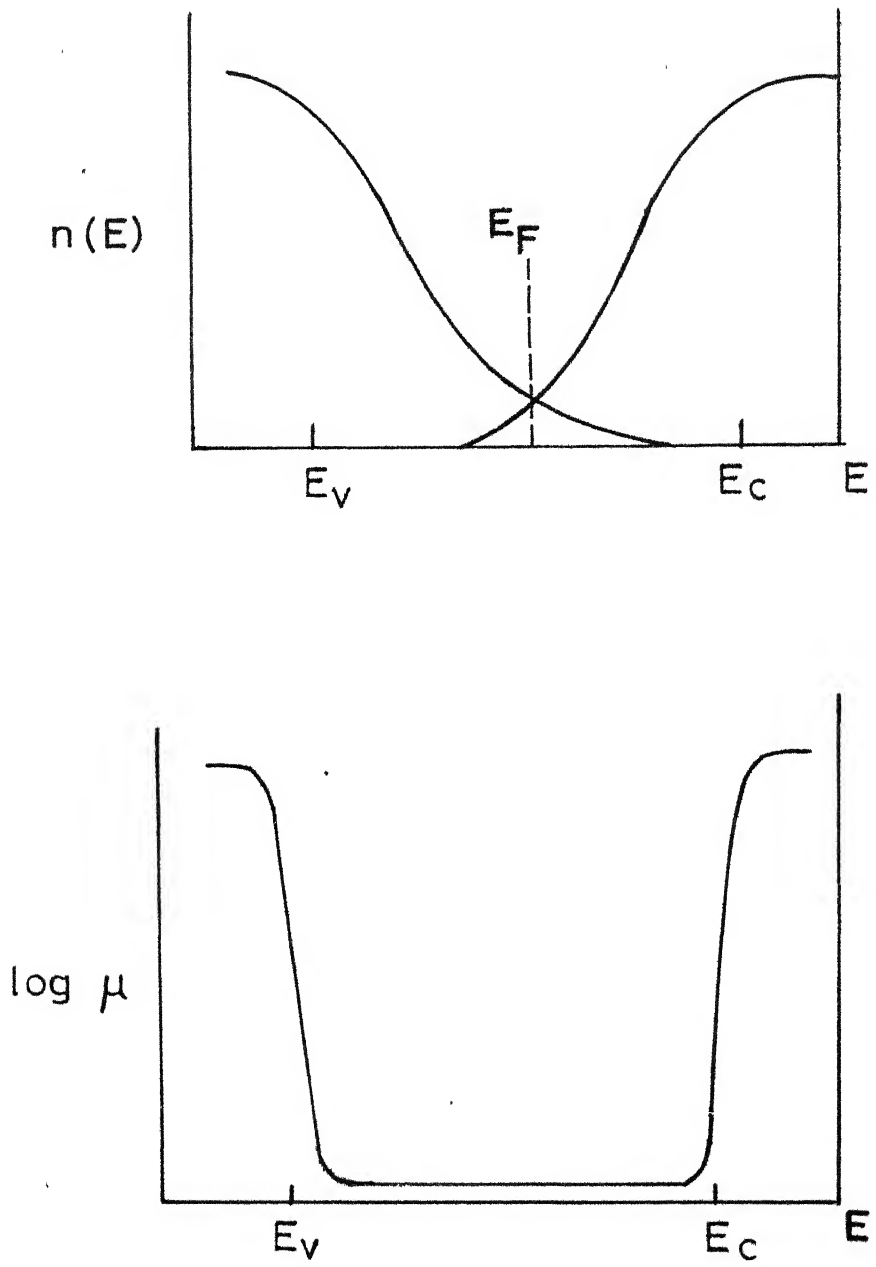

FIG. 1.2 THE MOBILITY GAP

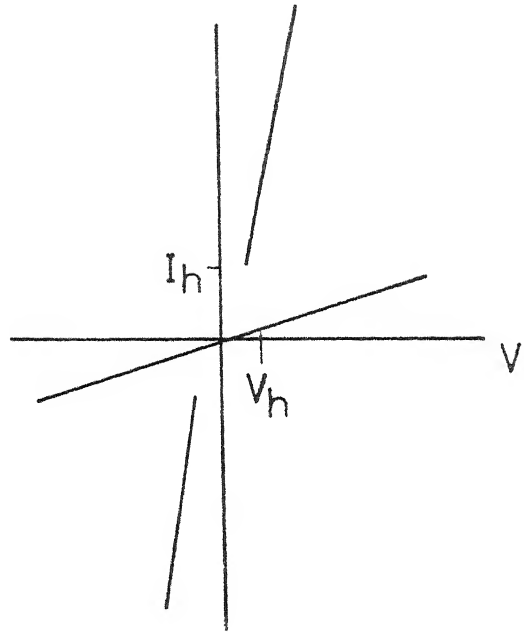

(a) THRESHOLD SWITCHING

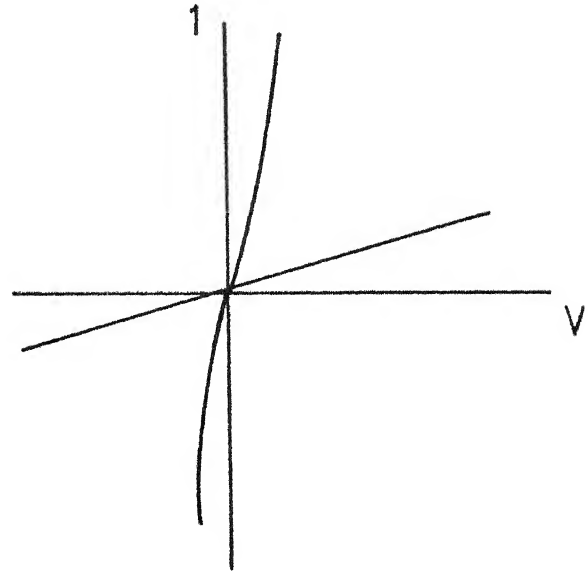

(b) MEMORY SWITCHING

FIG 1 3 CLASSIFICATION OF SWITCHING CHARACTERISTIC

CHAPTER II

STATEMENT OF THE PROBLEM

It has been established that glasses in the system, Na_2O-B_2O_3-Bi_2O_3-SiO_2 show memory switching. The purpose of this investigation is to study the effect of crystallisation of the glasses in order to be able to establish some sort of model for the on-state and off-state conductivity of the quarternary glass system. The five compositions studied are given in Table 3.1. The following observations, were made on these glasses.

(1) Variation of resistivity of these glasses with temperature. Both virgin glasses and glasses crystallised under heat treatment were studied.

(2) Study of X-ray diffraction pattern of crystallised glasses in order to identify the crystalline phase .

(3) Study of X-ray diffraction pattern of the identified phase to cross-check results.

(4) Variation of resistivity with temperature of this phase.

(5) Differential thermal analysis is studies on the glasses.

CHAPTER III

EXPERIMENTAL DETAILS

3.1 Base Glass Preparation

The glasses were prepared using reagent grade materials. Starting materials were: Na_2CO_3, K_2CO_3, SiO_2, H_3BO_3, Bi_2O_3. These were mixed carefully in a mortar using acetone. The quantities required to give the correct mole percent were added. The dry mixture was transferred into alumina crucibles and heated in an electrically heated furnace with globar rods. Melting temperatures ranged from 1000°C to 1300°C. After the melting temperature was reached the glass was allowed to homogenise for half an hour. The molten glass, free from bubbles was poured quickly into aluminium moulds kept at room temperature. It was then transferred into another furnace preheated to 500°C and annealed for 5 to 6 hrs. The furnace was then cooled slowly. The samples were stored in a dessicator.

The composition of the different glasses made is shown in Table 3.1. One mole percent K_2O was added in all the glasses to reduce the melting temperature.

Table 3.1: Compositions (mole %) of the Glasses Studied

Glass No.	SiO_2	B_2O_3	Bi_2O_3	Na_2O	K_2O
1	60	29	9	1	1
2	60	27	9	3	1
3	60	25	9	5	1
4	60	23	9	7	1
5	60	20	9	10	1

3.2 Crystallisation of the Glasses

To crystallise the glasses, virgin glasses were heated in an electrically heated furnace. The crystallisation temperature was carefully controlled. The time of the heat treatment was noted.

3.3 Specimen Preparation for Resistivity Measurements

For bulk resistivity measurements, the samples were cast into circular discs about 1 cm. in diameter. These samples were then polished to reduce the thickness to about 1 mm. Both virgin glass samples and crystallised glass samples were made. For polishing, silicon-carbide powder of different mesh numbers (120, 240, 400,

600 and 800) were used. The specimens were then coated with gold on both sides. Gold was evaporated onto the glass samples under high vacuum conditions. The samples were then mounted in a sample holder, the details of which are illustrated in Figure 3.1.

3.4 Resistivity Measurements

Resistivity measurements on all the samples were made in the temperature range 100°C to 400°C. The sample was mounted in the sample holder and the entire assembly kept in a kanthol wire wound furnace. Temperatures were carefully controlled using a temperature controller circuit. A General Radio Electrometer 1230-A and ECIL Picoammeter were used to measure current in the circuit. At every temperature, the current versus voltage across the specimen was measured over a decade of voltage and the sample resistance was calculated from the slopes of the linear V-I plots. The schematic diagram for the circuit is shown in Figure 3.2.

3.5 Preparation of Samples for X-Ray Diffraction Studies

The bulk glass samples were crushed to a fine powder. The powder was sieved so that the particle size was 53 microns.

3.6 Resistance Measurements on $Bi_2O_3.3B_2O_3$ Sample

The sample was prepared using reagent grade chemicals (B_2O_3 as boric acid and Bi_2O_3 as the oxide). The chemicals were mixed well together. The sample was treated at 150°C and 250°C for two hours each after mixing and powdering. It was then powdered till 31 micron and pellets were made using a pressure of 20,000 psi. The sample was treated then at 350°C for 4 hours. The pellets were again powdered and sieved to 31 microns. The pellets were made again. These were treated at 450°C for 10 hours.

The pellets were then polished. Using silicon carbide powder to about 1 mm thickness. Silver electrodes were applied on both sides by painting silver dag (made by NPL, India). Copper wires were fixed on silver electrodes using silver cement. To dry the cement the specimen was fired in an oven at 100°C to one hour. After the cement dried, the specimen was sandwiched between two glass slides using araldite.

For resistance measurements the schematic circuit diagram is shown in Figure 3.3.

For high temperature measurements, the sample was introduced into an electrically heated furnace operated by a temperature controller circuit. The sample was placed in a metallic tube.

For measurements below room temperature, the set-up is shown in Figure 3.4. Liquid nitrogen was taken in a 5 litre dewar. The sample was kept in a glass tube about 1 metre long. The liquid nitrogen was kept in the dewar, at the base of which was kept a heating coil wound around mica. Different rates of evaporation of nitrogen were obtained by heating the coil. The evaporating nitrogen cooled the sample. Different rates of evaporation gave different steady temperatures. The circuit employed for resistance measurement was the same as that in Figure 3.3.

3.7 Sample Preparation for D.T.A. Analysis

The glasses were powdered to 53 micron size. The powder was kept in a ceramic crucible. The analysis was made in the temperature range 0-1000°C. The rate of heating was 10°C/min.

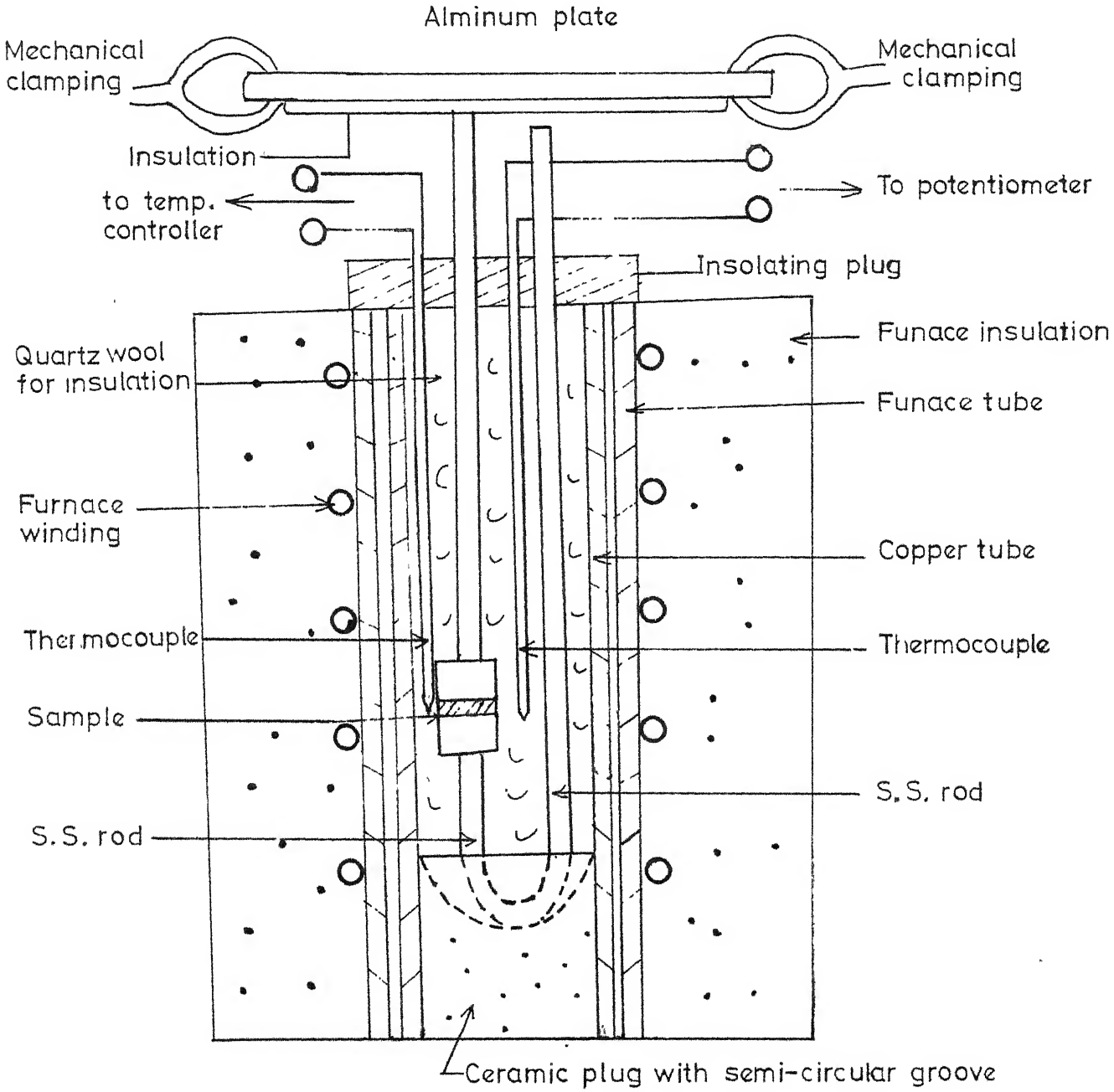

FIG. 3.1 SAMPLE HOLDER FOR RESISTIVITY MEASUREMENTS

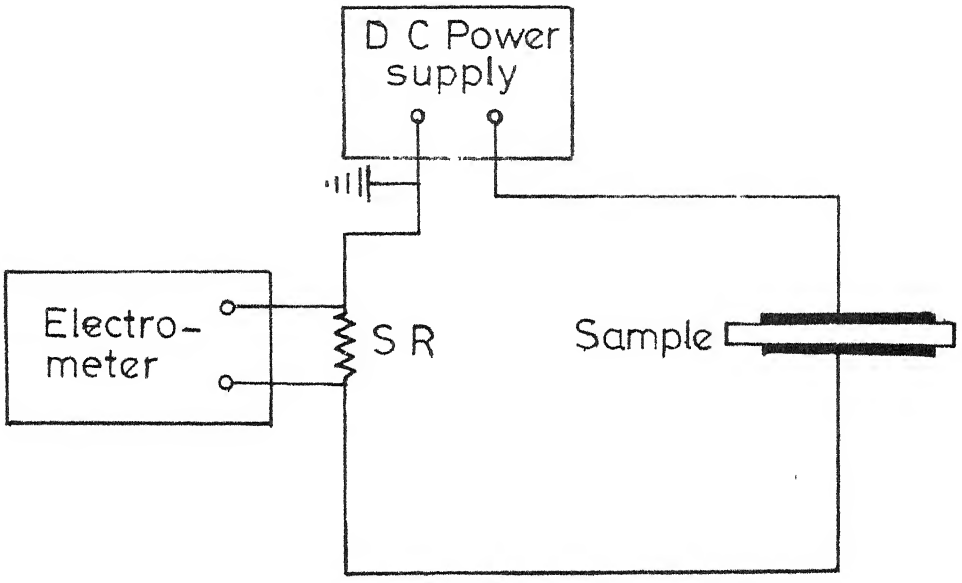

FIG. 3.2 SCHEMATIC CIRCUIT DIAGRAM FOR RESISTIVITY MEASUREMENT

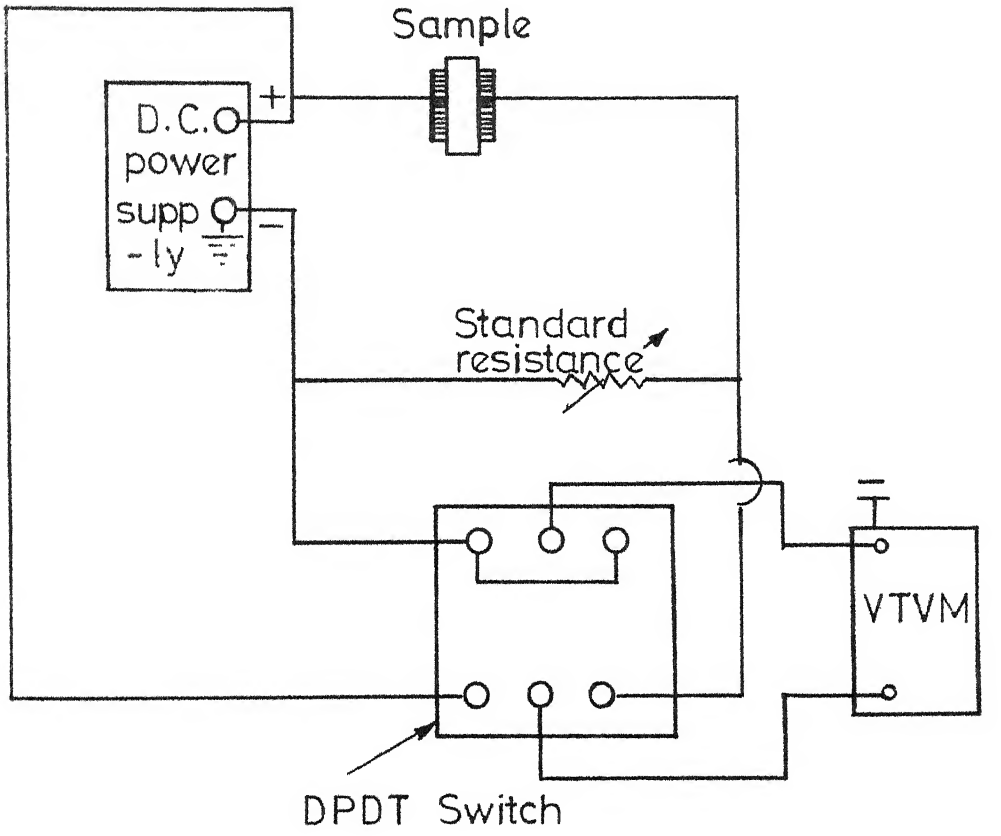

FIG.3.3 CIRCUIT DIAGRAM FOR RESISTIVITY MEASUREMENT WITH V T V M

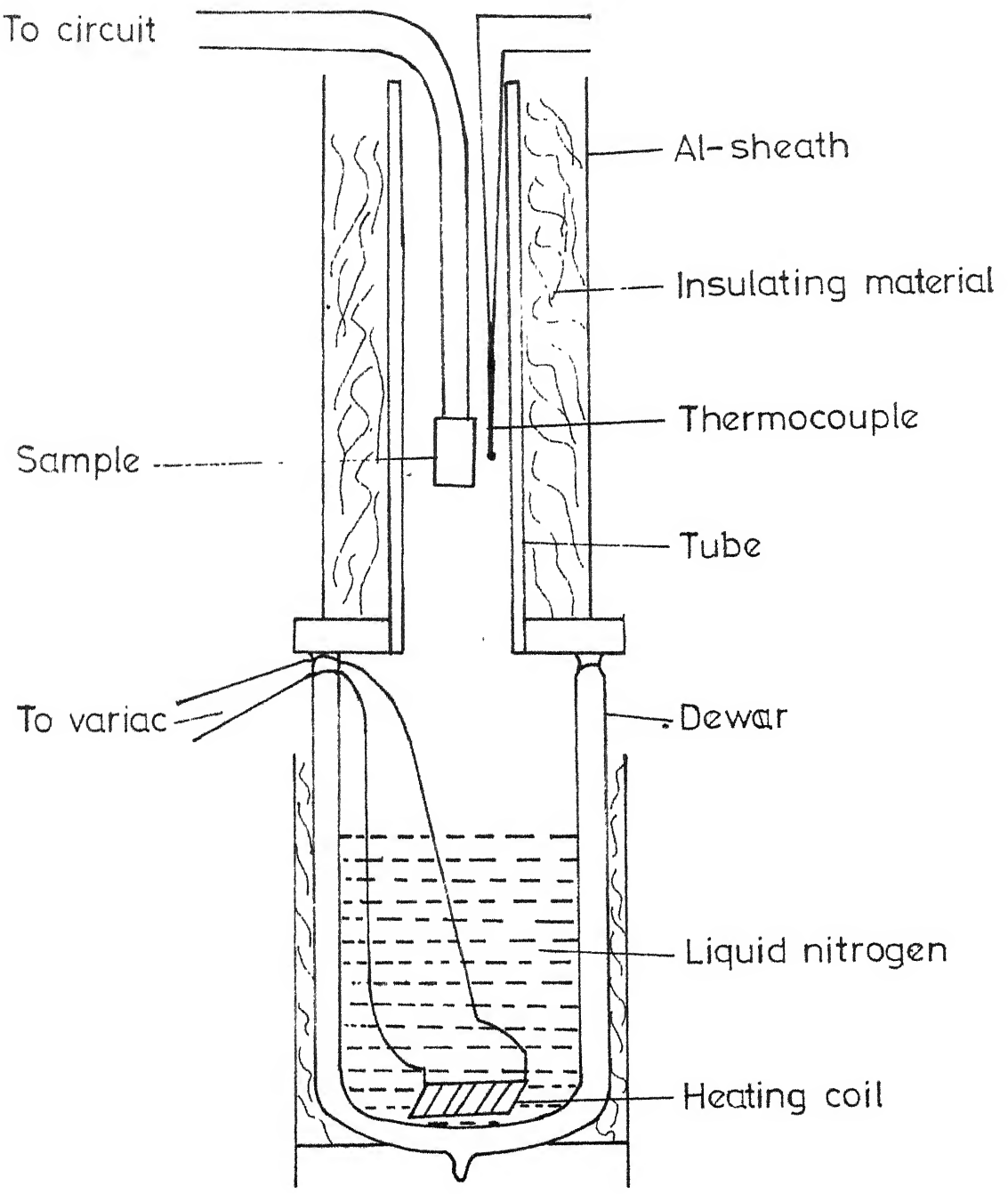

FIG.3.4 SETUR OF LOW TEMPERATURE RESISTIVITY MEASUREMENT

CHAPTER IV

RESULTS

4.1 Resistivity Measurements on Glasses

The V-I characteristics of the glasses studied were obtained as linear plots. The resistances at each temperature were obtained as the slopes of these plots.

The compositions studied are listed below in Table 4.1 and the glasses will be referred to by their numbers in this chapter.

Table 4.1: Compositions (mole %) Glasses Studied

Glass No.	SiO_2	B_2O_3	Bi_2O_3	Na_2O	K_2O
1	60	29	9	1	1
2	60	27	9	3	1
3	60	25	9	5	1
4	60	23	9	7	1
5	60	20	9	10	1

The logarithm of resistivity as a function of inverse temperature of virgin glasses no. 1, 3, 4 and 5 are

plotted in Figures 4.1, 4.2, 4.3 and 4.4 respectively. Class no. 1 was partially crystallised in preparation.

Resistance measurements were taken from 100°C to 400°C. Measurements were started at a temperature much higher than room temperature to avoid effects due to absorption of moistures as bismuth glasses tend to absorb moisture rapidly.

Resistivity plots of samples no. 1 and 3 (refer to Figure 4.1 and 4.2) show a peculiar behaviour. The plots are linear in the high temperature and low temperature ranges. In the middle temperature range the plot shows a dip. This could be due to a structural change in the glassy phase of these glasses. The dip of glass sample no. 1 occurs at roughly 270° this can be correlated to an endothermic peak obtained for this sample at around 310° in its DTA curve (Figure 4.15).

Glasses no. 4 and 5 do not show any such dip. But are smooth over the entire temperature range (refer Figures 4.3 and 4.4). The curve for glass no. 4 shows a slight discontinuity at around 280° which can be correlated to an endothermic peak in its DTA curve (Figure 4.16) at around 280°.

The activation energies are calculated using the relationship

$$\sigma = \sigma_o \cdot \exp(-\frac{E}{kT})$$

where σ is the d.c. conductivity and E is the activation energy. These are tabulated in Table 4.2.

In the high temperature range the values indicate ionic conductivity. The activation energy is found to decrease with increase in sodium content of the glasses consistent with Stevel's model of ionic conductivity.

In the low temperature range however, the low value of activation energy obtained in glasses no. 3 and 5 is indicative of electronic conduction. Neugebauer and Webb have shown that the activation energy for electron hopping between conducting islands with a diameter r is given by e^2/kr where e is the electronic charge and k is the dielectric constant of the surrounding medium. Assuming a value of k = 6 (23) the value of r calculated is r = 80 $\mathring{A}$.

Log ρ versus 1/T for the crystallised glasses are plotted in Figures 4.5, 4.6 and 4.7 for glasses no. 2, 3 and 4 respectively. The heat treatments given were:

Glass No.	Temperature, °C	Hours
2	660	12
3	666	30
4	648	12

The activation energies obtained for crystallised glasses no. 2 and 3 in the high temperature showed ionic conductivity. In glass no. 3 the plot obtained is linear throughout the temperature range and showed no decrease in activation energy with decrease in temperature. This is ascribed to some sort of hysteresis effect due to the heat treatment whereby the characteristics of conduction in the high temperature are retained in the low temperature range also.(see Table 4.2).

4.2 X-Ray Diffraction Data

Powder diffraction patterns for crystallised glasses no. 1, 2 and 3 and virgin glasses no. 1 and 2 are plotted in Figure 4.8. The pattern for the virgin glasses is fairly flat, indicating that the peaks obtained in the crystallised glasses are due to the crystallisation.

Table 4.2: List of Activation Energies in the Glasses Studied

Glass no.	Activation energy (eV)		
	High temperature range	Intermediate temperature range	Low temperature range
1	1.4	0.86	-
3	0.72	0.4	0.13
4	0.57	0.57	-
5	0.41	0.72	0.13
Crystallised glasses			
2	0.78	0.78	-
3	0.70	0.70	-
4	-	0.25	-

X-ray data obtained for crystallised glass no. 1 was analysed for the d values to identify the crystalline phase. Predominant d values were correlated to d values of possible phases that could be present using the Davey Index in the Index to the Powder Diffraction File (ASTM). The predominant d values of $Bi_2O_3.3B_2O_3$ and $3Bi_2O_3.5B_2O_3$ were found to match with the d values obtained.

$Bi_2O_3.3B_2O_3$ was synthetically prepared in the lab and its powder diffraction pattern taken . This is compared with the pattern of crystallised glass no. 1 in Figure 4.9. The patterns are found to match fairly well.

The 'd' values of the crystallised glass specimen, those for synthetically prepared $Bi_2O_3.3B_2O_3$ and the 'd' values obtained by Levis and McDaniel (26) are compared in Table 6.8. They are found to compare , fairly well.

4.3 Resistivity Measurements on $Bi_2O_3.3B_2O_3$ Specimens

Two samples were prepared of $Bi_2O_3.3B_2O_3$ of the same composition and heat treatments in two separate batches. They will be referred to as sample no. 1 and 2.

Figure 4.10 plots the OFF-state resistance characteristics of sample no. 1. For V less than 1 volt the characteristic is linear giving a resistance of 7×10^6 ohm. Between 1 and 2.5 volts the sample shows unstable behaviour. At 2.5 volts the sample switched to the ON-state.

Figure 4.11 shows the ON-state characteristic of sample no. 1. The V-I plot is linear and the resistance obtained is 9.4×10^2 ohms.

The low temperature characteristics of this sample were taken from room temperature to -100°C. The V-I plots obtained were linears and resistance values were calculated from the slopes. Figure 4.12 plots log of resistivity versus inverse temperature for this sample. Resistivity is found to decrease with decrease in temperature except for a peak at around 0°C which can be due to some inherent instability in the sample.

The TCR in the low temperature range is around 1100 $ppm°K^{-1}$ which is about one-third the value of metallic bismuth. Hence some sort of metallic conductivity is indicated.

ON-state characteristics for sample no. 2 were obtained in the temperature range 0-200°C. The V-I plot was linear only below 1 volt (Figure 4.13). Above that the plot was non-linear showing electrode effects. Resistivity values were obtained from the linear regions and these are plotted in Figure 4.14. Not much can be obtained from these plots because the resistivity values may not be very accurate due to the very small linear region of the plots.

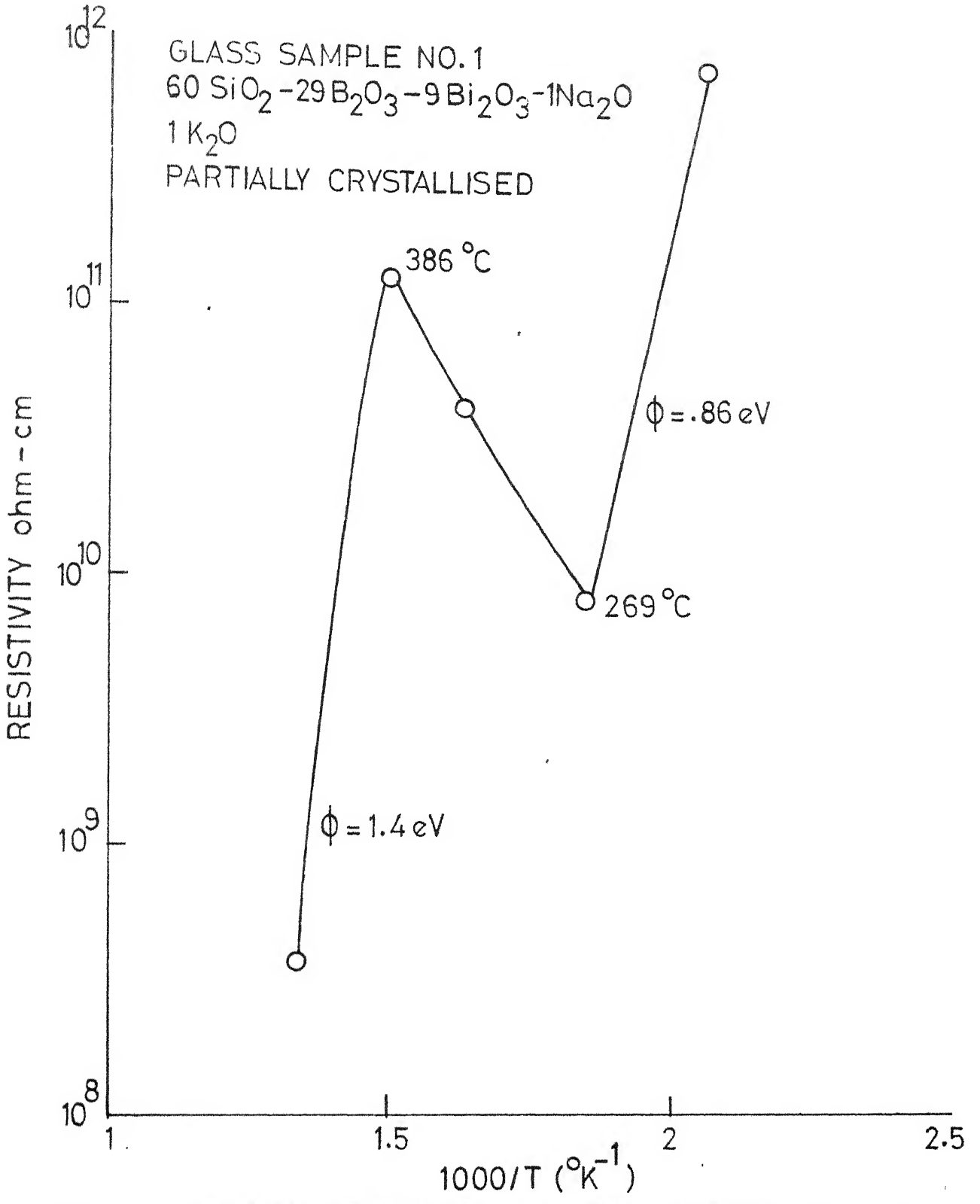

FIG.4.1 VARIATION OF RESISTIVITY WITH INVERSE OF ABSOLUTE TEMPERATURE FOR GLASS NO. 1

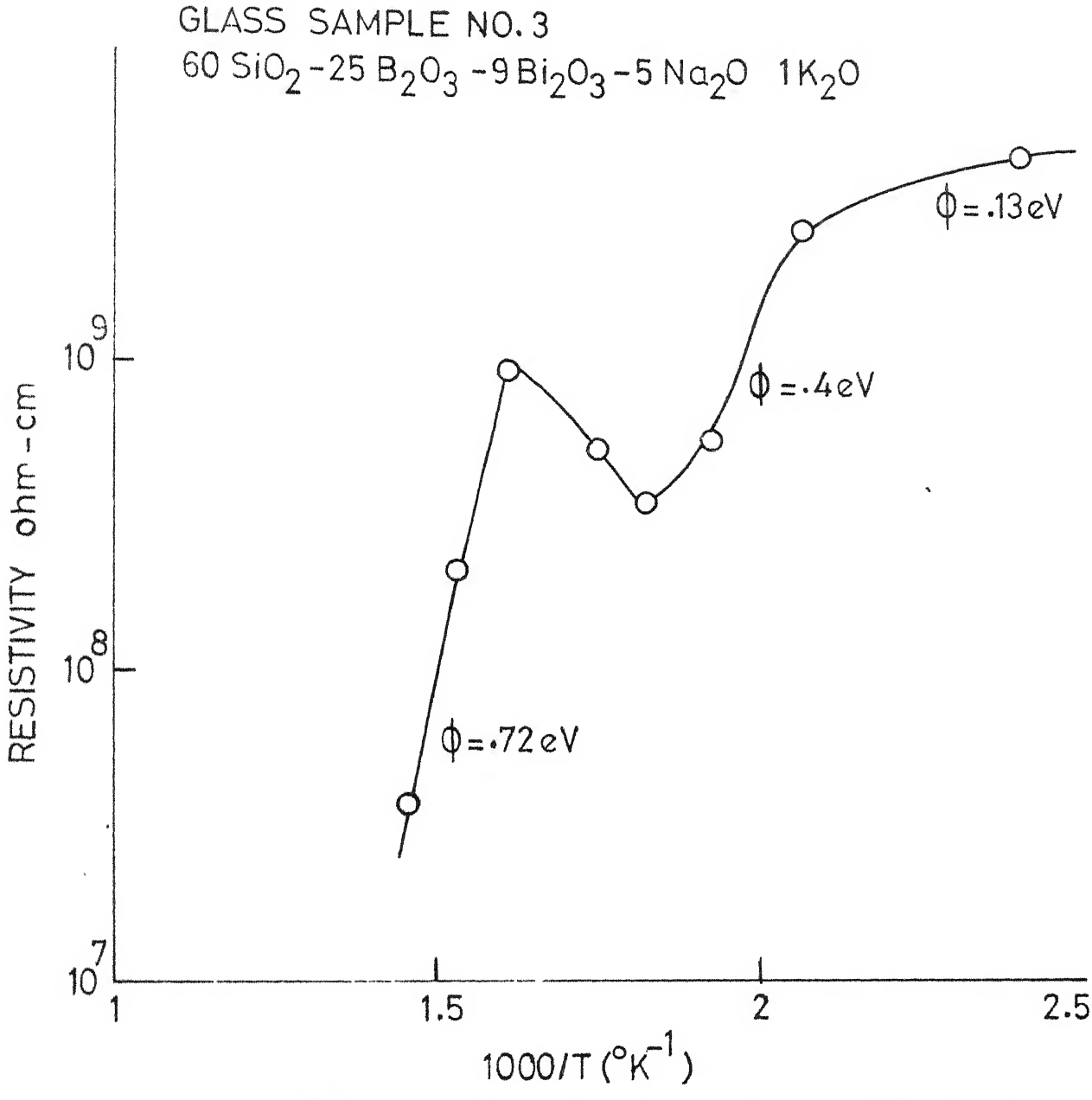

FIG. 4.2 VARIATION OF RESISTIVITY WITH INVERSE OF ABSOLUTE TEMPERATURE OF GLASS NO. 3

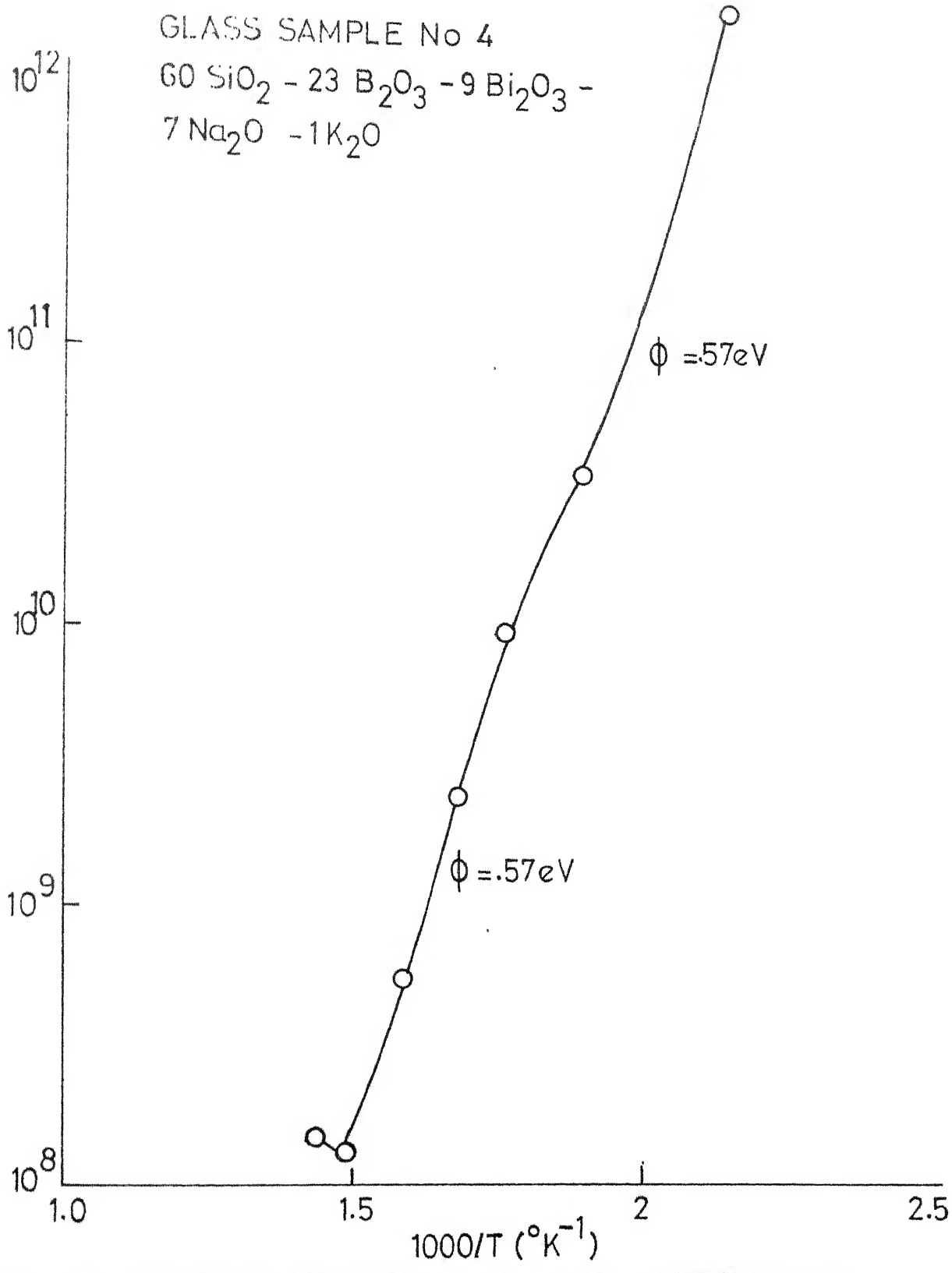

FIG 4 3 VARIATION OF RESISTIVITY WITH INVERSE OF ABSOLUTE TEMPERATURE FOR GLASS NO. 4

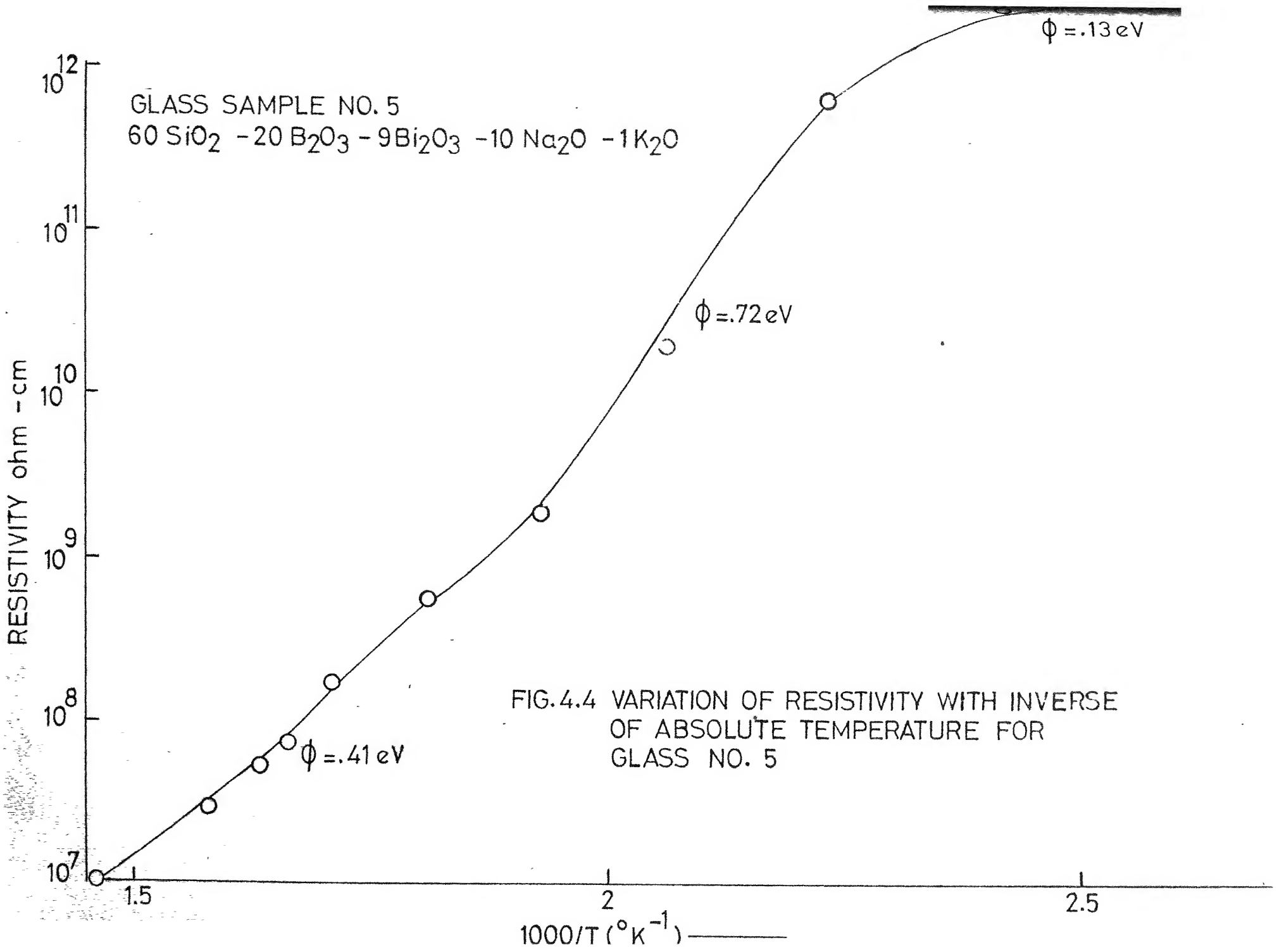

FIG. 4.4 VARIATION OF RESISTIVITY WITH INVERSE OF ABSOLUTE TEMPERATURE FOR GLASS NO. 5

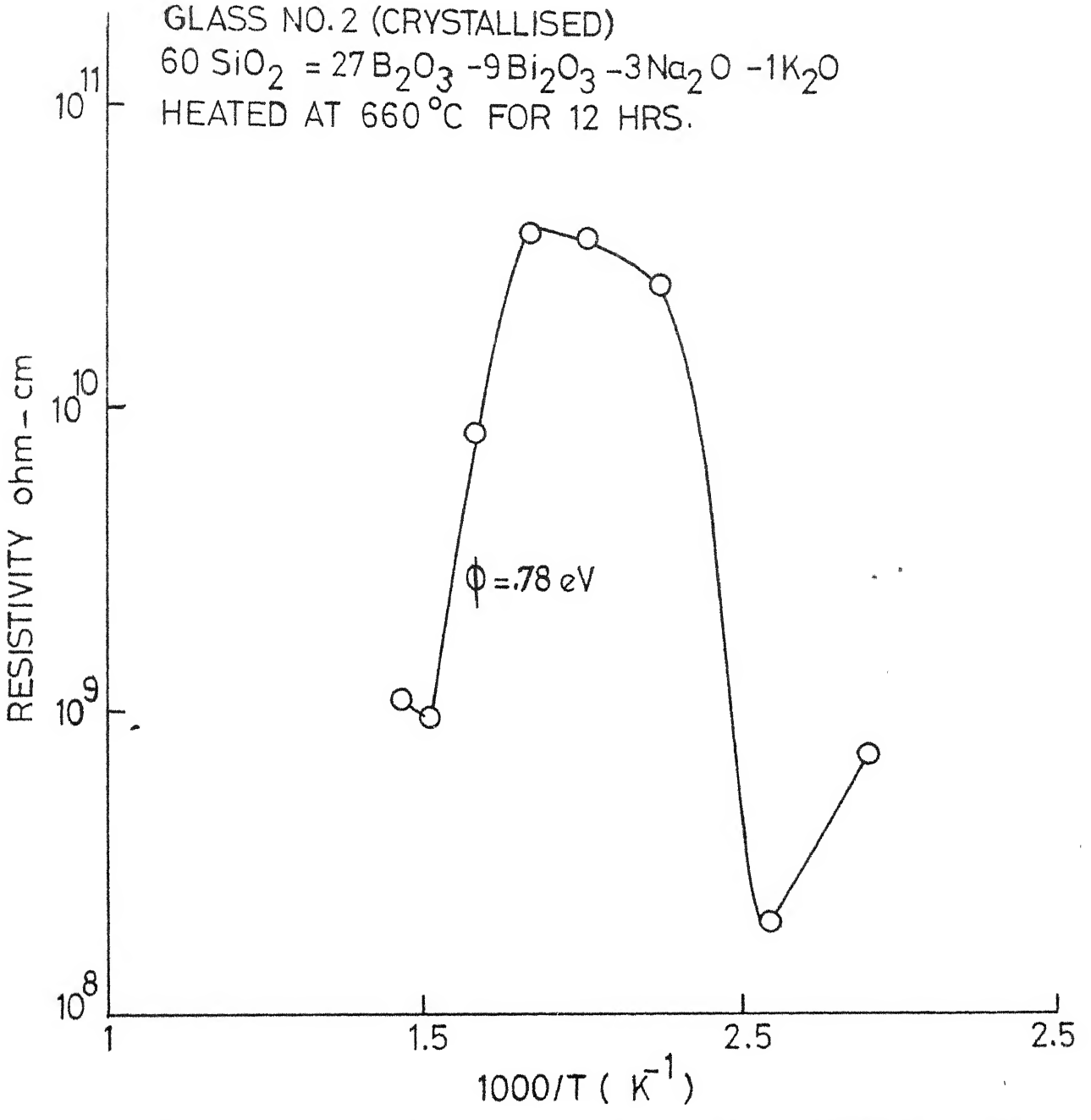

FIG.4.5 VARIATION OF RESISTIVITY WITH INVERSE OF ABSOLUTE TEMPERATURE FOR CRYSTALLISED GLASS NO. 2

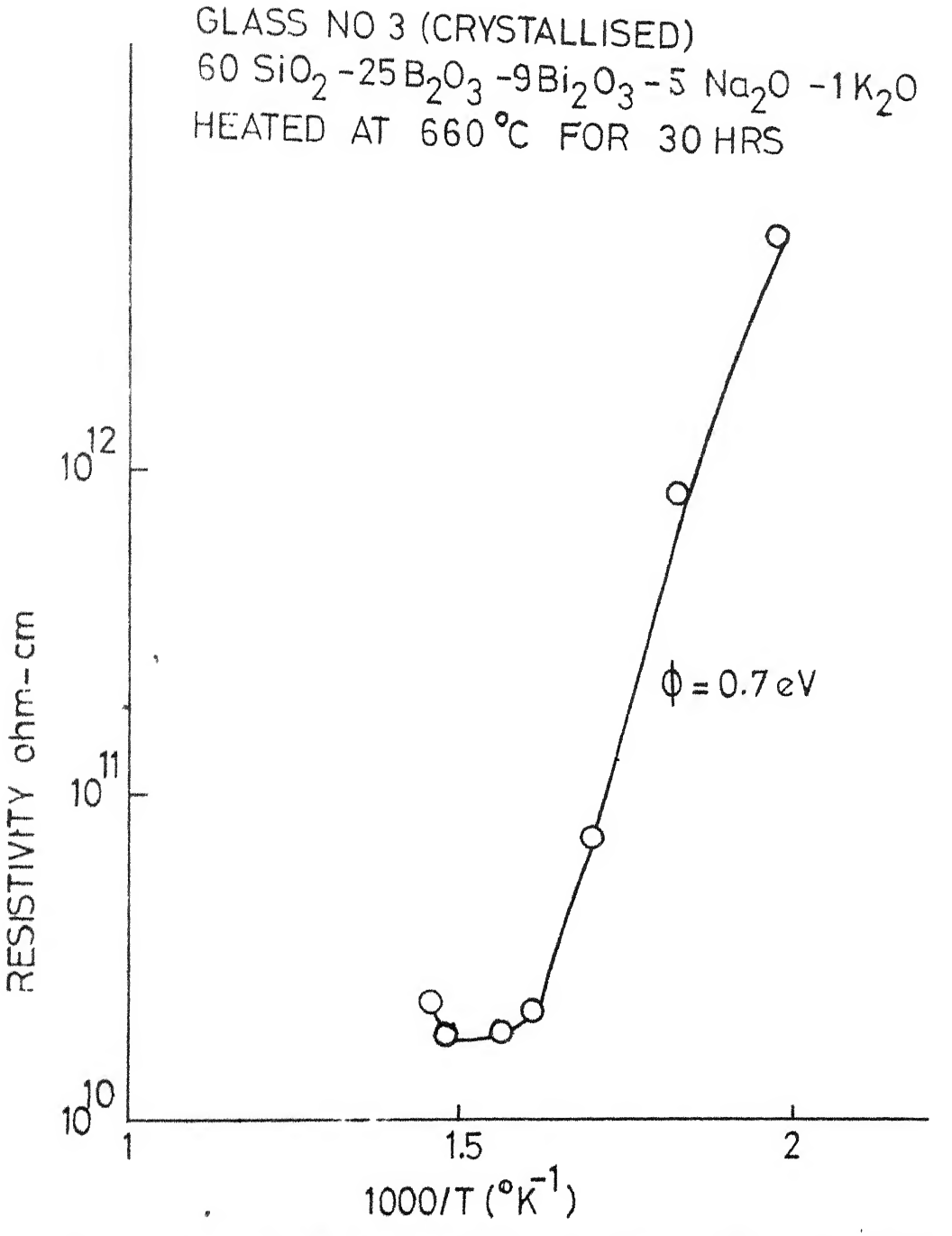

FIG.4.6 VARIATION OF RESISTIVITY WITH INVERSE OF ABSOLUTE TEMPERATURE FOR CRYSTALLISED GLASS NO. 3

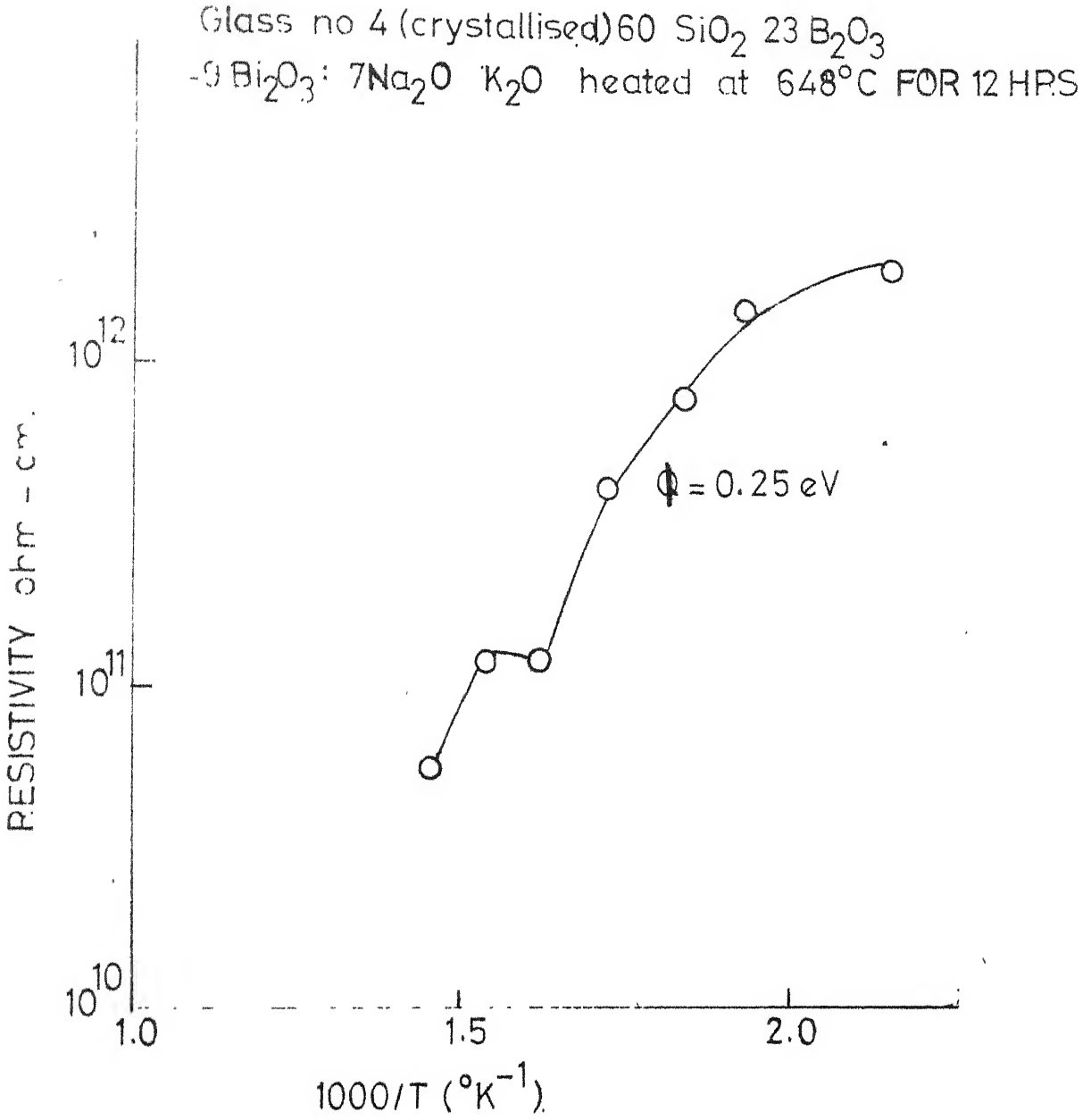

FIG. 4.7 VARIATION OF RESISTIVITY WITH INVERSE OF ABSOLUTE TEMPERATURE FOR CRYSTALLISED GLASS NO. 4

CHAPTER V

CONCLUSIONS AND PROPOSALS FOR FURTHER WORK

The X-ray diffraction data obtained shows conclusively that the crystalline phase in the glass is a $Bi_2O_3.B_2O_3$ compound. The exact role that this phase plays in the switching of the glass is difficult to say conclusively at this stage.

The resistivity characteristic of this phase shows a switching of the same order of magnitude as the glass itself is found to show. That the crystalline phase itself is inherently switching indicates that it might act as a catalyst to the glass switching, but whether the precipitation of the phase itself causes switching is difficult to ascertain. Two factors which do not support the theory that the formation of a crystalline phase in the glassy matrix causes switching are

(1) the fact that switching has been shown to occur in the glass at low temperatures. It is difficult to envisage a mechanism by which at such low temperatures localised regions in the glass attain temperatures high enough for the formation of the crystalline phase (temperature $\sim$ 600-700°C).

(2) the switching time is $\sim$ 10 micro seconds. This time seems to be too small for the formation of a stable crystalline phase.

One possibility is that in localised positions in the glassy matrix, due to favourable conditions regions are formed which have compositions very similar to the $Bi_2O_3 \cdot 3B_2O_3$ phase, and electron hopping between these states gives rise to the OFF-state. The ON-state is obtained by formation of metallis bismuth filaments between these crystalline phases. What role the switching of the crystalline phase itself shows is difficult to show. The fact that the $Bi_2O_3 \cdot B_2O_3$ phase shows metallic conduction supports this fact.

Another possibility is that bismuth particles are precipitated in the crystalline phase and the crystalline phase acts as an intermediate between the glassy phase and the bismuth phase i.e. the situation is a complicated three-phase situation.

It is difficult at this stage to conclude exactly what part crystallisation plays in the switching property of the glass. All that can be said is that the crystalline phase identified itself shows interesting electrical

behaviour and may be an interesting system for further investigation.

Proposals for further work along this line are

(1) detailed electrical characterisation of the crystalline phase.

(2) electron micrograph studies of the glass obtained by varying the temperature could show interesting aspects of the phase changes. It may be possible to identify the phase exactly which gives rise to the switching behaviour.

CHAPTER VI

LIST OF TABLES

Table 6.1: Resistivity Data of Glass No. 1

$60SiO_2 - 29B_2O_3 - 9Bi_2O_3 - 1Na_2O - 1K_2O$ (mole %)

Thickness of specimen = 0.14 cm

Area of electrode = 0.9 cm^2

Temperature (°K)	Resistivity (ohm-cm)
484	7.59×10^{11}
537	8.04×10^{9}
610	3.22×10^{10}
659	1.22×10^{11}
746	2.66×10^{8}

Table 6.2: Resistivity

Data for Glass No. 3

$60SiO_2 - 25B_2O_3 - 9Bi_2O_3 - 5Na_2O - 1K_2O$ (mole %)

Thickness of specimen = 0.15 cm

Electrode area = 1.2 cm^2

Temperature, (°K)	Resistivity (ohm-cm)
417	4.64×10^8
480	1.7×10^8
518	5.5×10^7
546	2.46×10^7
569	5.08×10^7
616	9.6×10^7
648	2.1×10^7
685	3.84×10^6

Table 6.3: Resistivity Data of Glass No. 4

$60SiO_2 - 23B_2O_3 - 9Bi_2O_3 - 7Na_2O - 1K_2O$ (mole %)

Thickness of sample = 0.14 cm

Electrode area = 0.89 cm^2

Temperature(°K)	Resistivity (ohm-cm)
468	1.67×10^{12}
527	3.54×10^{10}
561	9.92×10^{9}
596	1.5×10^{9}
628	5.47×10^{8}
671	1.32×10^{8}
695	1.48×10^{8}

Table 6.4: Resistivity Data for Glass No. 5

$60SiO_2 - 20B_2O_3 - 9Bi_2O_3 - 10Na_2O - 1K_2O$ (mole %)

Thickness of sample = 0.14 cm

Electrode area = 4.8 cm^2

Temperature (°K)	Resistivity (ohm-cm)
396	3.42×10^{12}
416	2.8×10^{12}
447	6.84×10^{11}
487	1.98×10^{10}
495	2.05×10^{9}
518	1.8×10^{9}
275	5.34×10^{8}
309	1.71×10^{8}
604	7.87×10^{7}
614	5.13×10^{7}
630	3.11×10^{7}
673	1.02×10^{7}

Table 6.5: Resistivity Data for Glass No. 2 Crystallised $60SiO_2 - 27B_2O_3 - 9Bi_2O_3 - 3Na_2O - 1K_2O$ (mole %) treated at 660°C for 12 hours.

Sample thickness = 0.14 cm

Electrode area = 2.58 cm^2

Temperature (°K)	Resistivity (ohm-cm)
452	7.36×10^8
489	2.36×10^8
534	2.63×10^{10}
568	3.68×10^{10}
598	3.79×10^9
631	8.54×10^9
656	9.2×10^8
682	11×10^8

Table 6.6: Resistivity Data for Glass No. 3 Crystallised at 660°C for 30 hours

$60SiO_2 - 25B_2O_3 - 9Bi_2O_3 - 5Na_2O - 1K_2O$ (mole %)

Thickness of sample = 0.15 cm

Area of electrode = 3.3 cm^2

Temperature (°K)	Resistivity (ohm-cm)
464	12.3×10^{12}
504	5.5×10^{12}
549	8.58×10^{11}
588	7.33×10^{10}
629	2.13×10^{10}
646	1.97×10^{10}
677	1.81×10^{10}
689	2.39×10^{10}

Table 6.7: Resistivity Data for Glass No. 4 Crystallised at 648°C for 12 hours

$60SiO_2 - 23B_2O_3 - 9Bi_2O_3 - 7Na_2O - 1K_2O$ (mole %)

Thickness of specimen = 0.15 cm

Area of electrode = 1.3 cm^2

Temperature (°K)	Resistivity (ohm-cm)
464	2.32×10^{12}
515	1.74×10^{12}
543	8.28×10^{11}
581	4.35×10^{11}
619	1.22×10^{11}
650	1.3×10^{11}
683	5.73×10^{10}

Table 6.8: Comparison of 'd' Values Obtained in the X-ray Diffraction Pattern of

(1) Glass sample no. 1. Crystallised at 700°C for 10 hours

$60SiO_2 - 29B_2O_3 - 9Bi_2O_3 - 1Na_2O - 1K_2O$ (mole %)

(2) Synthetically prepared. $Bi_2O_3 - 3B_2O_3$

(3) 'd' values obtained by Levin and McDaniel for the system. $Bi_2O_3 - 3B_2O_3$ (26)

d (Å) of Glass No. 1 crystallised	d (Å) of prepared sample $Bi_2O_3 - 3B_2O_3$	d (Å) and I/I_o of $Bi_2O_3 - 3B_2O_3$ obtained by Levin and McDainel	
6.324	6.4188	6.25	42
-	6.0320	-	-
4.271	4.271	4.04	78
3.935	3.899	-	-
3.708	3.619	3.66	33
3.452	3.452	3.42	20
3.350	3.303	-	-
3.209	3.255	3.168	100
3.187	3.187	-	-

Continued...

Table 6.8 (continued)

3.121	3.10	3.129	22
2.885	2.849	2.707	15
2.636	2.698	2.691	20
2.536	2.529	-	-
2.368	2.392	2.497	11
2.211	2.249	2.087	10
-	2.058	2.076	15
-	-	2.053	7
1.973	1.973	1.987	36
-	-	1.966	18
1.933	1.957	1.952	10
1.896	1.873	1.837	33
1.860	1.840	-	-
1.721	1.746	1.746	8
-	1.664	1.602	10
1.585	1.590	1.590	5
-	-	1.586	16
-	-	1.544	7

Table 6.9: Resistivity Data for $Bi_2O_3 - 3B_2O_3$.

Sample no. 1. Low temperature measurement

Thickness of specimen = 0.165 cm

Electrode area = 1.65 cm^2

Temperature (°K)	Resistivity (ohm-cm)
293	7.5×10^3
278	7.5×10^3
257	7.5×10^3
247	8.0×10^3
229	6.6×10^3
214	6.6×10^3
174	6.3×10^3

Table 6.10: Resistivity Data for $Bi_2O_3 - 3B_2O_3$

Sample no. 2. High temperature measurement

Electrode area = 1.28 cm^2

Sample thickness = 0.17 cm

Temperature (°K)	Resistivity (ohm-cm)
434	2.39×10^3
410	3.528×10^3
394	3.03×10^3
369	3.46×10^3

REFERENCES

(1) M.H. Cohen, H. Fritzche and S.R. Ovshinsky, Phys. Rev. Letters, 22, 1065, 1969.

(2) N.F. Mott, Advances in Physics, 16, 49, 1967; Phil. Mag., 22, 7, 1970.

(3) N.F. Mott and E.A. Davis, Electronic Processes in Non-Crystalline Materials, Clarendon Press, Oxford, 1971, Ch. 2.

(4) P.W. Anderson, Phys. Rev., 109, 1492, 1958.

(5) J.T. Edmond, J. Non-Cryst. Solids, 1, 39, 1968.

(6) C. Hilsom, Electronic Materials, Hannay Colombo, Plenum Press, New York, Proceedings of the third International Conference on Materials Science held in Italy, Sept. 4-15, 1972.

(7) P.L. Baynton, H. Rawson and J.E. Stanworth, J. Electrochem. Soc., 104, 237, 1957.

(8) O.A. Esin and V.L. Ziazev, Z. Neorg. Khim., 11, 1998, 1957.

(9) N.F. Mott, J. Non-Cryst. Solids, 1, 1 (1969).

(10) I.G. Austin and N.F. Mott, Advan. Phys., 18, 41, (1969).

(11) Elec. Conduction in Ceramics and Glass, Tallan.

(12) S.R. Ovshinsky, Phys. Rev. Letters, 21, 1450, 1968.

(13) S.R. Ovshinsky and H. Fritzche, IEEE Transactions on Electronic Devices, Feb. 1973.

(14) A.D. Pearson, J. Non-Cryst. Solids, 2, 1, (1970).

(15) K.W. Boer, Phys. Stat. Solidi (a), 4, 571, 1971.

(16) J.J. O'Dwyer, J. Electrochem. Soc., 116, 239, 1969.

(17) A.D. Pearson, IBM J. Res. Develop., 13, 510, 1969.

(18) S.R. Ovshinsky, J. Non-Cryst. Solids, 2, 99, 1970.

(19) D. Eaton, J. Am. Ceram. Soc., 116, 239, 1969.

(20) H.K. Henisch and R.W. Pryor, Solid State Electronics, 14, 765, 1971.

(21) C.B. Thomas, and J.R. Bosnell, Phil. Mag., 27, 665, 1973.

(22) D. Chakravorty, J. of Non-Cryst. Solids, 15, 191-198, 1974.

(23) D. Chakravorty and C.S. Murthy, J. Phys. P: Appl. Phys., Vol. 8, 1975 (G. Britain).

(24) D. Chakravorty and R. Bhatnagar, to be published.

(25) C.A. Neugebauer and M.B. Webb, J. Appl. Phys., 33, 74, 1962.

(26) E.M. Levin and C.L. McDaniel, J. Am. Ceram. Soc., Vol. 45, No. 8, Aug. 1962.

(27) S.M. Ohlberg and D.W. Strickler, J. Am. Ceram. Soc., 1962, p. 170.

(28) R.H. Doremus, Glass Science, John Wiley and Sons, 1973.

(29) N.F. Mott, Phil. Mag., 19, 835, 1969.

(30) N.F. Mott, Phil. Mag., 24, 911, 935, 1971.

(31) N.F. Mott and E.A. Davis, Electronic Processes in Non-Crystalline Materials, Oxford University Press, London, 1971.

(32) M.H. Onnar, E.L. Hammsy and A.M. Bishay, Proc. of IXth Inter. Glass Congress, Paris, 1971.

(33) Proceedings of Int. Conf. on Amorphous and Liquid Semiconductor, J. Non-Cryst. Solid, May 1969 and Sept. 1969.

(34) A.D. Pearson et.al., Advances in Glass Technology, Plenum Press, New York, 1972.